"Eddy Resolving" Observation of the North Pacific Subtropical Mode Water

EITAROU OKA,* TOSHIO SUGA,+,# CHIHO SUKIGARA,+,@ KATSUYA TOYAMA,+ KEISHI SHIMADA,&,** AND JIRO YOSHIDA&

* *Atmosphere and Ocean Research Institute, The University of Tokyo, Kashiwa, Japan*
+ *Department of Geophysics, Graduate School of Science, Tohoku University, Sendai, Japan*
# *Research Institute for Global Change, Japan Agency for Marine-Earth Science, and Technology, Yokosuka, Japan*
@ *Hydrospheric Atmospheric Research Center, Nagoya University, Nagoya, Japan*
& *Department of Ocean Sciences, Tokyo University of Marine Science and Technology, Tokyo, Japan*
** *Institute of Low Temperature Science, Hokkaido University, Sapporo, Japan*

(Manuscript received 12 May 2010, in final form 27 December 2010)

ABSTRACT

Hydrographic data obtained by high-resolution shipboard observations and Argo profiling floats have been analyzed to study the mesoscale structure and circulation of the North Pacific Subtropical Mode Water (STMW). The float data show that in the late winter of 2008, STMW having a temperature of approximately 18.8°, 17.7°, and 16.6°C formed west of 140°E, at 140°–150°E, and east of 150°E, respectively, in the recirculation gyre south of the Kuroshio Extension. After spring, the newly formed STMW gradually shift southward, decreasing in thickness. Simultaneously, the STMWs of 16.6° and 17.7°C are gradually stirred and then mixed in terms of properties. In late fall, they seem to be integrated to form a single group of STMWs having a temperature centered at 17.2°C. Such STMW circulation in 2008 is much more turbulent than that in 2006, which was investigated in a previous study. The difference between the two years is attributed to the more variable state of the Kuroshio Extension in 2008, associated with stronger eddy activities in the STMW formation region, which enhance the eddy transport of STMW.

High-resolution shipboard observations were carried out southeast of Japan at 141°–147°E in the early fall of 2008. To the south of the Kuroshio Extension, STMW exists as a sequence of patches with a horizontal scale of 100–200 km, whose thick portions correspond well to the mesoscale deepening of the permanent pycnocline. The western (eastern) hydrographic sections are occupied mostly by the 17.7°C (16.6°C) STMW, within which the 16.6°C (17.7°C) STMW exists locally, mostly at locations where both the permanent pycnocline depth and the STMW thickness are maximum. This structure implies that the STMW patches are transported away from their respective formation sites, corresponding to a shift in the mesoscale anticyclonic circulations south of the Kuroshio Extension. Furthermore, 20%–30% of the observed STMW pycnostads have two or three potential vorticity minima, mostly near temperatures of 16.6° and 17.7°C. The authors presume that such a structure formed as a result of the interleaving of the 16.6° and 17.7°C STMWs after they are stirred by mesoscale circulations, following which they are vertically mixed to form the 17.2°C STMW observed in late fall. These results indicate the importance of horizontal processes in destroying the vertically uniform structure of STMW after spring, particularly when the Kuroshio Extension is in a variable state.

1. Introduction

In the North Pacific Ocean, a deep mixed layer is formed on both the southern and the northern sides of the Kuroshio Extension in late winter (e.g., Ladd and Thompson 2000; Suga et al. 2004; Oka et al. 2007, 2011), and remains in the subsurface in the following seasons as two prominent isopycnal layers known as the Subtropical Mode Water (STMW; Masuzawa 1969) and the Central Mode Water (CMW; Nakamura 1996; Suga et al. 1997), respectively. In the following winter, part of the formed mode waters is entrained into the mixed layer, affecting the persistence of winter sea surface temperature anomalies (e.g., Alexander and Deser 1995; Hanawa and Sugimoto 2004; Sugimoto and Hanawa 2005), whereas the remaining part is subducted into the permanent pycnocline and then advected away from its formation regions. In association with the formation and circulation, the anomalies of temperature, salinity, and potential

Corresponding author address: Eitarou Oka, Atmosphere and Ocean Research Institute, The University of Tokyo, 5-1-5, Kashiwanoha, Kashiwa-shi, Chiba 277-8564, Japan.
E-mail: eoka@aori.u-tokyo.ac.jp

DOI: 10.1175/2011JPO4501.1

vorticity are transmitted downward to the subsurface layers as well as horizontally as the volume and properties of the mode waters formed every winter change from year to year (e.g., Suga and Hanawa 1995a; Yasuda and Hanawa 1997; Hanawa and Kamada 2001; Suga et al. 2003). Therefore, the two mode waters are believed to cause the fluctuations in the permanent pycnocline structure of the North Pacific subtropical gyre and to have a certain influence on the climate and its variability in the Pacific region, through the basin-scale transport of temperature anomalies (e.g., Latif and Barnett 1994; Gu and Philander 1997) and the generation of the Subtropical Countercurrent (Kubokawa and Inui 1999; Kubokawa 1999; Aoki et al. 2002; Kobashi et al. 2006, 2008). Moreover, they possibly affect the long-term climate variability by regulating the oceanic uptake of atmospheric CO_2 (e.g., Bates et al. 2002).

The recent completion of a global array of temperature/salinity profiling floats under the international Argo program (Roemmich et al. 2001) has enhanced our understanding of the formation and circulation of STMW and CMW and their interannual variability, compared to the last century, during which the observational studies on water masses relied mainly on climatological data and limited repeat section data. The formation and subduction of CMW were investigated using the float data in 2003–08 by Oka et al. (2011). To the north of the Kuroshio Extension, two regions of deep winter mixed layers extend zonally at 33°–39°N and 39°–43°N from the east coast of Japan to ~160°W, corresponding to the formation regions of the lighter and denser varieties of CMW (Tsujino and Yasuda 2004; Oka and Suga 2005), respectively. From the eastern part of each formation region east of 170°E, where the winter mixed layer gradually becomes shallow eastward/downstream, the respective varieties of CMW are subducted into the permanent pycnocline and are then advected anticyclonically in the subtropical gyre toward the western boundary.

A greater number of studies have been performed using the float data on the formation and circulation of STMW and their interannual variation (Uehara et al. 2003; Oka and Suga 2003; Pan and Liu 2005; Qiu and Chen 2006; Qiu et al. 2006, 2007; Oka 2009; Sugimoto and Hanawa 2010). Among these, Oka (2009) examined the formation and circulation of STMW over the entire distribution region in 2006. Thick STMW is formed in late winter in the recirculation gyre south of the Kuroshio Extension, which zonally extends north of 28°N, between 135°E and 180°. The recirculation gyre consists of several anticyclonic circulations, in each of which STMW with a characteristic temperature is formed. By tracking these temperatures, the STMW circulation after spring can be visualized. In 2006, a large part of the newly formed, thick STMW is continually trapped in each anticyclonic circulation until late fall, remaining in the formation region. From this stagnant pool of STMW, some portion gradually seeps into the southern region and is then transported southwestward by subsurface currents, as far as the western boundary. Such STMW circulation differs from the traditional climatology-based picture that the thick body of STMW is advected southwestward as the season progresses (e.g., Suga and Hanawa 1995b). At present, however, the degree to which the observed STMW circulation in 2006 applies to the other years is not clear.

The last decade also witnessed significant progress in the modeling of currents and water masses in the North Pacific (e.g., Hasumi et al. 2010; Masumoto 2010). Recently, the high-resolution ocean general circulation models of Rainville et al. (2007) and Nishikawa et al. (2010) demonstrated the highly variable distribution of STMW caused by high mesoscale activity in the Kuroshio Extension region (e.g., Qiu 2002). In addition, Nishikawa et al. (2010) quantitatively examined the role of mesoscale eddies in the transport and subduction of STMW. At the southern boundary of the STMW formation region, anticyclonic eddies transport STMW southward, at a right angle to the westward mean flow. This occurs in two ways: 1) the southward migration of an eddy that traps STMW and 2) eddy mixing (i.e., a combination of the southward transport of STMW from the formation region in the eastern part of an eddy and the northward transport of water with a relatively high potential vorticity from the southern region in the western part of the eddy). Because of this southward transport, STMW crosses the front of the winter mixed layer depth (Kubokawa and Inui 1999; Kubokawa 1999; Nishikawa and Kubokawa 2007) and is thereby subducted into the permanent pycnocline. Such eddy subduction contributes to approximately half of the total STMW subduction rate (Nishikawa et al. 2010).

Although the data from the Argo floats also imply mesoscale STMW distribution (Uehara et al. 2003; Pan and Liu 2005; Qiu et al. 2006; Oka 2009), the standard float density of one per three degree square is too low to obtain a synoptic STMW distribution with a resolution comparable to the high-resolution models. Therefore, we conducted a high-resolution hydrographic survey in the western North Pacific southeast of Japan in fall 2008 during the KH-08-3 cruise leg 2 of R/V *Hakuho-maru*. Two meridional lines at 143° and 146°E and three shorter zonal lines at 27°30′, 30°, and 34°N were occupied (Fig. 1) using a conductivity–temperature–depth–oxygen profiler ($CTDO_2$) at intervals of 30′ or 1° in latitude/longitude and an expendable conductivity-temperature-depth profiler (XCTD) or an expendable bathythermograph (XBT) at

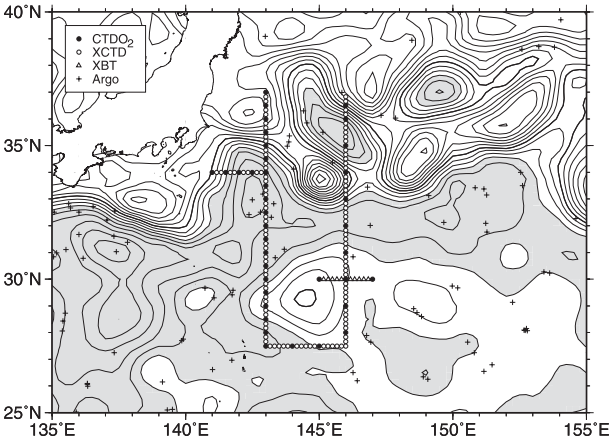

FIG. 1. Locations of $CTDO_2$ (closed circles), XCTD (open circles), and XBT (triangles) stations of the KH-08-3 cruise leg 2 from 22 Oct to 4 Nov 2008, and Argo float observations (crosses) during the cruise period. The background contours represent the altimetric sea surface height on 29 Oct 2008. The contour is drawn at an interval of 10 cm, with a thick one at 220 cm and a shaded region for >250 cm.

10′ intervals, along with other physical/biogeochemical instruments. By analyzing the data from $CTDO_2$/XCTD/XBT as well as those from the Argo floats, we investigate in this paper the mesoscale structure and circulation of STMWs that have been inadequately investigated in previous observational studies.

2. Data and processing

We used temperature T, salinity S, and dissolved oxygen data obtained by $CTDO_2$ (Sea-Bird Electronics, Inc.; Model 9-plus; 38 stations), XCTD (Tsurumi Seiki Co. Ltd.; 108 stations), and XBT (Tsurumi Seiki Co. Ltd.; T-7 type; 10 stations) from 22 October to 4 November 2008, during the KH-08-3 cruise leg 2 of R/V *Hakuhomaru* (Fig. 1). The S data from particular XCTD probes had a systematic bias, and were calibrated as is explained in the appendix. An S profile at each XBT station along 30°N was estimated using the observed T profile at the same station and the T–S relations at nearby CTD stations. From these observed and estimated data, potential temperature (θ), in situ water density (ρ), potential density (σ_θ), and apparent oxygen utilization (AOU) were calculated.

Zonal and meridional geostrophic velocities (u, v; positive eastward and northward) across each hydrographic section were computed using a reference level of 1000 dbar or the maximum observation pressure near 800 dbar (only at XBT stations along 30°N) after ρ was horizontally smoothed along the section using a three-point Hanning filter with weights of 0.25, 0.5, and 0.25 (specifically, ρ at a depth of j dbar at ith station, $\rho_{i,j}$, was replaced by $0.25 \times \rho_{i-1,j} + 0.5 \times \rho_{i,j} + 0.25 \times \rho_{i+1,j}$). Then, using the available u or v, potential vorticity (Q) was calculated on the basis of the definition:

$$Q = -\frac{f + \partial v/\partial x}{\rho}\frac{\partial \sigma_\theta}{\partial z}, \tag{1}$$

for the zonal sections and

$$Q = -\frac{f - \partial u/\partial y}{\rho}\frac{\partial \sigma_\theta}{\partial z}, \tag{2}$$

for the meridional sections, where f is the Coriolis parameter, x and y are the cross- and along-stream coordinates (positive eastward and northward, respectively), and z is the vertical coordinate (positive upward). Here, the horizontal velocity shear ($\partial v/\partial x$, $\partial u/\partial y$) was estimated between adjacent hydrographic station pairs by letting Δx (Δy) be 10′ in longitude (latitude). The calculated magnitude of the relative vorticity relative to the planetary one ($|\partial v/\partial x/f|$, $|\partial u/\partial y/f|$) attains a maximum of 35% in the Kuroshio Extension; however, it is much smaller (generally, less than 10%) and negligible south of the Kuroshio Extension where STMW exists.

We also used T and S data obtained by Argo floats in the North Pacific in 2003–08. These floats drift freely at a predetermined parking pressure (typically, 1000 dbar), and conduct T–S measurements from an intermediate depth (2000 dbar) to near the sea surface (4 dbar) at a predetermined interval (10 days). The data collected at approximately 70–120 sampling pressures, with a typical interval of 5 dbar at depths shallower than 200 dbar, 10–25-dbar intervals at 200–1000 dbar, and 50–100-dbar intervals at deeper than 1000 dbar, are transmitted from the surfaced floats to satellites, and they are freely available within 24 h, after passing through the Argo real-time quality control (Argo Data Management Team 2009).

We downloaded the real-time quality-controlled float data from the ftp site of the Argo Global Data Assembly Center (see online at ftp://usgodae1.fnmoc.navy.mil/pub/outgoing/argo, ftp://ftp.ifremer.fr/ifremer/argo), and eliminated the defective T–S profiles such as those with measurements flagged as bad and those lacking intermediate layers for certain depths, according to the procedures of Oka et al. (2007). We then interpolated each T–S profile vertically on a 1-dbar grid using the Akima spline (Akima 1970), and calculated θ, σ_θ, and Q. In the Q calculation for the Argo data, the relative vorticity was disregarded.

We also used delayed-time sea surface height data merged from Ocean Topography Experiment (TOPEX)/Poseidon, *Jason-1*, *Jason-2, European Remote Sensing Satellite-1/2 (ERS-1/2)*, and *Envisat* altimeter observations,

produced by Ssalto/Duacs and distributed by Archiving, Validation, and Interpretation of Satellite Oceanographic data (AVISO; Ducet et al. 2000). The weekly data in 2008, provided on a 0.25° × 0.25° grid, were downloaded from the Web site of AVISO (see online at http://www.aviso.oceanobs.com).

In this study, STMW is defined in each $CTDO_2$/XCTD/XBT/Argo profile as the layer that has a Q value less than the critical value, with a minimum Q in the θ range of 16°–19.5°C, following the definition of Oka (2009). The low-Q layers with thickness less than 25 dbar and those existing only at depths less than 100 dbar are regarded as small-scale features and are excluded. STMW is considered to outcrop (not to outcrop) at the sea surface if its top is located at a depth less than (greater than) 10 dbar. Accordingly, such STMW is hereafter referred to as either outcropping or nonoutcropping STMW.

Within the low-Q layer of STMW, the core, defined by the Q minimum, is considered to be the least modified since the low-Q portion was formed, thereby best preserving the water properties at the time of formation. In the following part of the paper, a water property at the core (e.g., θ) is simply referred to as "core θ."

3. Large-scale STMW circulation in 2008

Before analyzing the one-time regional data from the KH-08-3 cruise leg 2, in this section, we use the Argo float data from 2008 to examine the large-scale STMW circulation over the entire distribution region, in comparison with that from 2006 presented in Oka (2009). For several years prior to 2008, the STMW thickness in the formation region decreases significantly, likely due to its decadal variability (Qiu and Chen 2006). If we define STMW using the same critical Q value of 1.5×10^{-10} m^{-1} s^{-1} as in Oka (2009), the thickness in May and June, averaged in three longitudinal ranges (140°–150°, 150°–160°E, and 160°–170°E) in the STMW formation region between the Kuroshio Extension and 28°N (following Fig. 12 in Oka 2009), decreases steadily from 2004 (167–192 dbar) to 2008 (83–131 dbar) by ~70 dbar. A similar decreasing trend during 2004–08 was presented by Sugimoto and Hanawa (2010) for the winter and summer STMW thicknesses in the northern part of the formation region north of 31°N. Because of this reduction, the STMW formed in the late winter of 2008 is so thin that if we define it using the critical Q value of 1.5×10^{-10} m^{-1} s^{-1}, only a small amount of it remains in the fall, when the KH-08-3 cruise leg 2 was conducted (not shown). Consequently, in the present study, we define the STMW in 2008 using a less severe critical value of 2×10^{-10} m^{-1} s^{-1}.

In the late winter of 2008, thick STMW is formed between the Kuroshio Extension and 28°N (Fig. 2a), a region similar to that seen in 2006 (Fig. 2b) and the preceding years (Oka 2009). Nonoutcropping STMW south of 28°N, presumably formed in previous winters, is mostly thinner than 150 dbar, forming a front of STMW thickness at the southern boundary of the formation region at ~28°N (Fig. 2a). Exceptionally, relatively thick STMW, thicker than 200 dbar, is found at 25°–28°N in April. This STMW is likely to be formed in the late winter of 2008 and then quickly transported southward.

After spring, the thick STMW gradually shifts southward while gradually losing its thickness, and is located at 24°–33°N in September–October. In November–December, it almost flattens between 21° and 33°N, except in the south of Japan where STMW thicker than 400 dbar remains in a strong anticyclonic recirculation (Figs. 2a,c). Such a temporal change in the STMW structure differs from that during 2003–06, when the newly formed, thick STMW does not shift southward, staying in the formation region until late fall (Figs. 2b,c; Oka 2009). It rather resembles the seasonal evolution of STMW in the climatological field (Suga and Hanawa 1995b).

The histogram of core θ for relatively thick STMW in May–June indicates that the STMW formed in the late winter of 2008 can be classified into three modes (Fig. 3a, top panel), in a similar manner to 2006 (Fig. 3b, top panel; Oka 2009) but much more clearly, thanks to the wider range of core θ. The three modes in 2008, namely, a warm mode with a core θ of 18.2°–19.1°C, a middle mode of 17.1°–18.2°C, and a cold mode of 16.4°–17.1°C, are mostly located west of 140°E, between 140° and 150°E, and east of 150°E in May–June, and they are probably formed in their respective regions in late winter (Fig. 4). The core θ of the three modes is still distinguishable in July–August, but the boundary between the two colder modes begins to blur in September–October, and the two modes seem to become integrated, forming a new mode in November–December (Fig. 3a). This differs from 2006, in which the core θ of the three modes changes little until late fall (Fig. 3b).

The STMW circulation after spring is also different between 2006 and 2008. In 2008, the middle and cold modes are gradually stirred as the season progresses, and they finally coexist with each other in November–December (Fig. 4). This suggests that the new mode is produced in late fall owing to the mixing of the middle and cold modes. In 2006, on the other hand, the three modes tend to be continually trapped in the respective anticyclonic circulations in the formation region, existing separately until late fall (Fig. 7 of Oka 2009). Note that the difference in the STMW circulation between the two years is not due to that in the critical Q value used for the STMW definition; the STMW circulation in 2006 (2008)

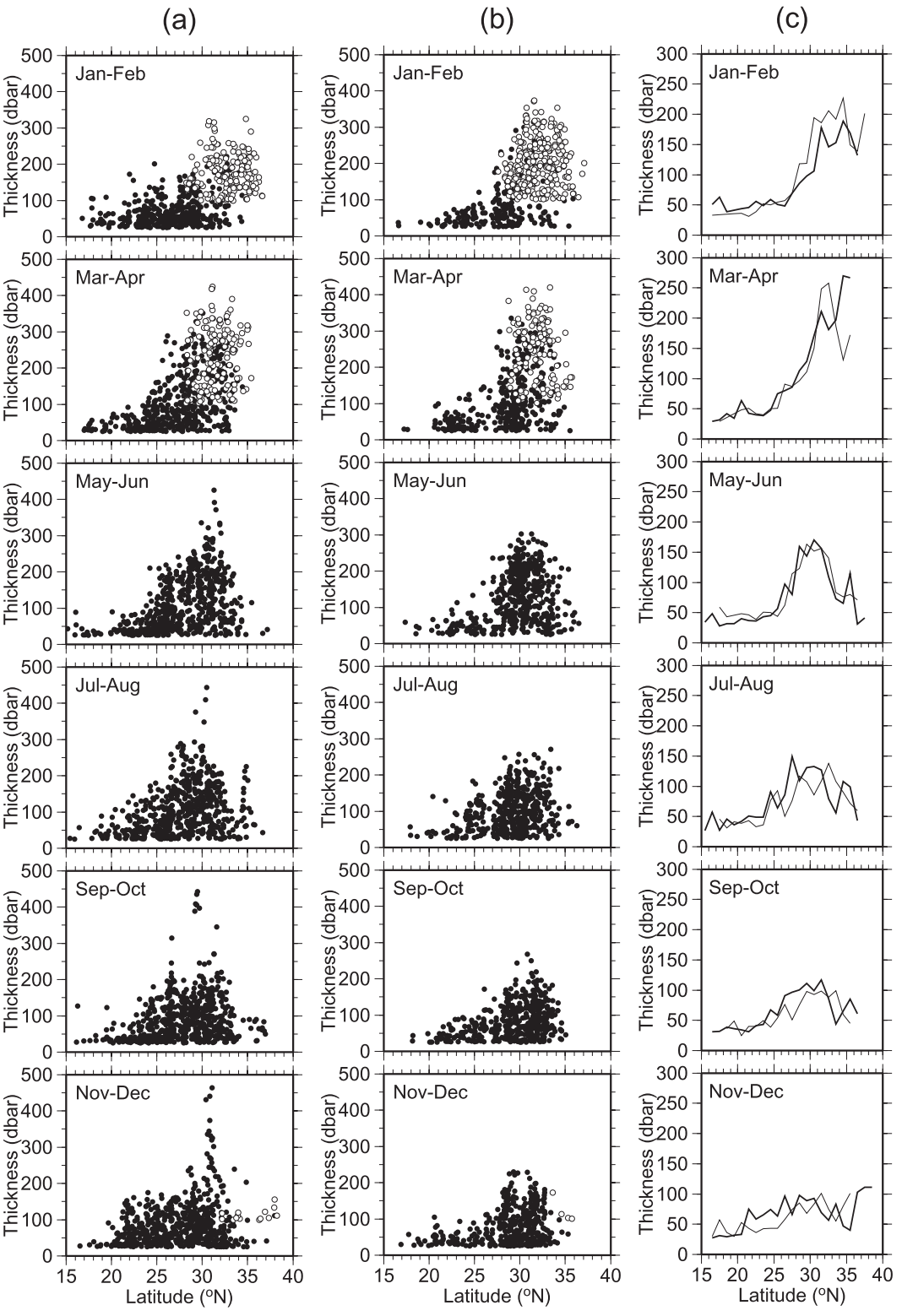

FIG. 2. Plots of STMW thickness against latitude from January–February through November–December in (a) 2008 and (b) 2006 (adapted from Oka 2009), based on Argo float data. The open (closed) circles denote outcropping (nonoutcropping) STMW. (c) Meridional variation of STMW thickness from January–February through November–December in 2008 (thick curve) and 2006 (thin curve) averaged for each 1° bin of latitude.

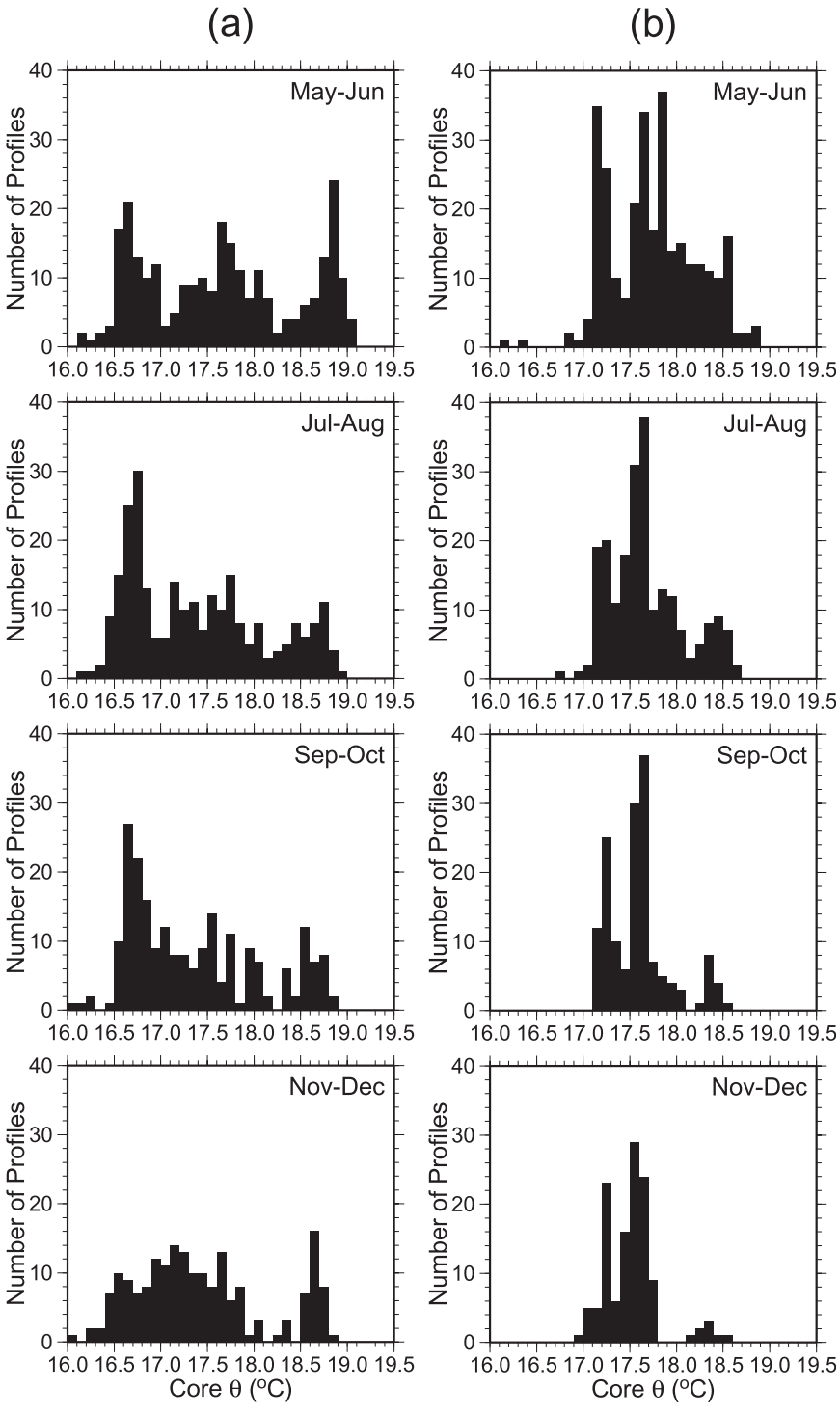

FIG. 3. Number of profiles with nonoutcropping STMW thicker than 100 dbar in each 0.1° bin of core θ from May–June through November–December in (a) 2008 and (b) 2006 (adapted from Oka 2009), based on Argo float data.

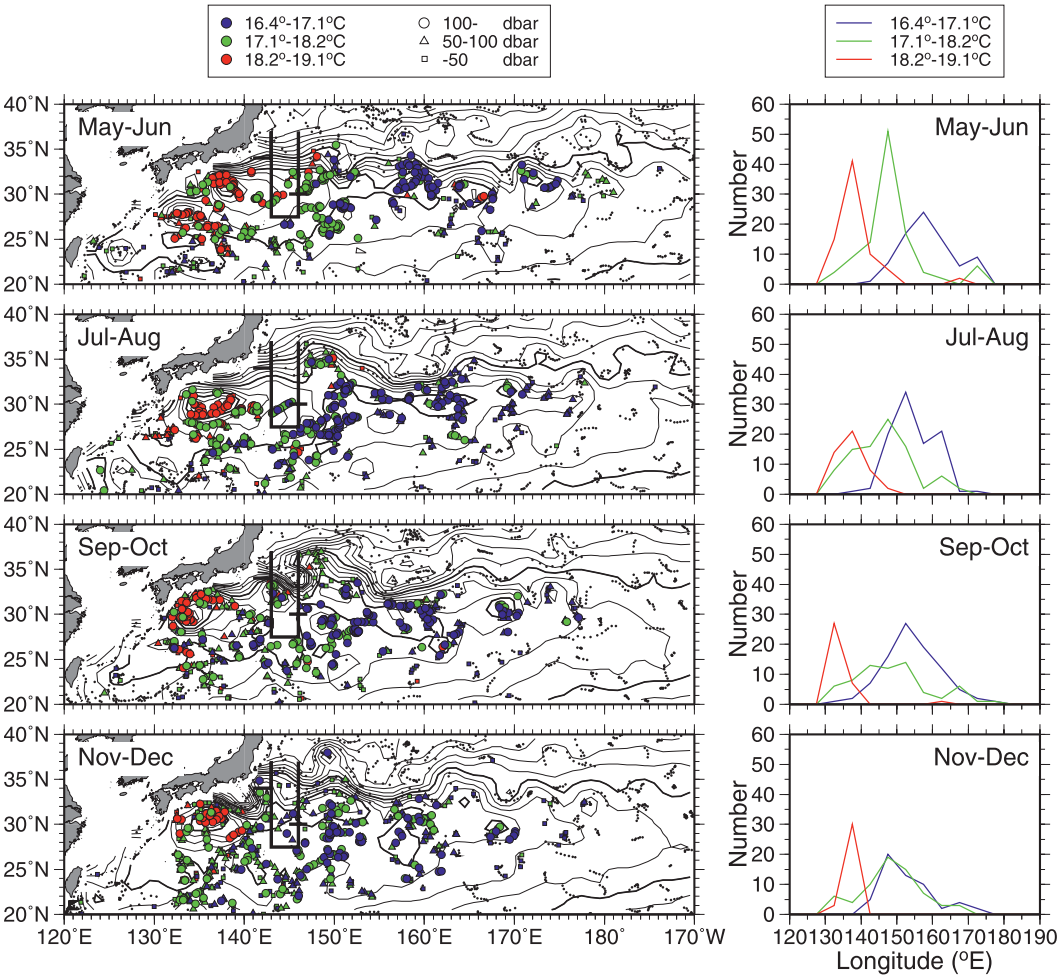

FIG. 4. (left) Distribution of nonoutcropping STMW with a core θ of 16.4°–17.1°C (blue symbols), 17.1°–18.2°C (green symbols), and 18.2°–19.1°C (red symbols) and geopotential anomaly at 250 dbar relative to 950 dbar ($m^2\ s^{-2}$; contours) from May–June through November–December in 2008, based on Argo float data. The symbol type denotes STMW thickness: greater than 100 dbar (circles), 50–100 dbar (triangles), and less than 50 dbar (squares). The black dots denote float observation points with STMW having the other core θ, those with outcropping STMW, and those without STMW. The geopotential anomaly at 250 dbar (average depth of the STMW core from spring through fall) was calculated from the float data using an optimal interpolation technique (Bretherton et al. 1976; see Oka 2009, for more details), and its contour is drawn at an interval of 0.5 $m^2\ s^{-2}$, with thick ones at 10, 12, and 14 $m^2\ s^{-2}$. The thick black lines denote the observation lines of the KH-08-3 cruise leg 2. (right) Number of profiles with nonoutcropping STMW thicker than 100 dbar located north of 25°N with a core θ of 16.4°–17.1°C (blue curve), 17.1°–18.2°C (green curve), and 18.2°–19.1°C (red curve) from May–June through November–December in 2008, counted for each 5° bin of longitude.

does not change essentially, even if STMW is defined using the critical value of 2.0 (1.5) $\times\ 10^{-10}\ m^{-1}\ s^{-1}$.

The observed difference in the STMW circulation between 2006 and 2008 is expected to be due to that in the flow field south of the Kuroshio Extension. On a decadal time scale, the Kuroshio Extension is alternately in stable and variable states with weak (or strong) eddy activity in the surrounding region during the former (or latter) period (Qiu and Chen 2005). It has been in the variable state since 2006, and exhibits the most variable path in 2008 (Figs. 5 and 6). The associated eddy activity in the STMW formation region, stronger in 2008 than in 2006, is believed to have caused the more turbulent STMW circulation during 2008.

4. Mesoscale structure of STMW southeast of Japan in fall 2008

In 2008, the Kuroshio Extension, in a highly variable state, meanders and fluctuates, occasionally detaching

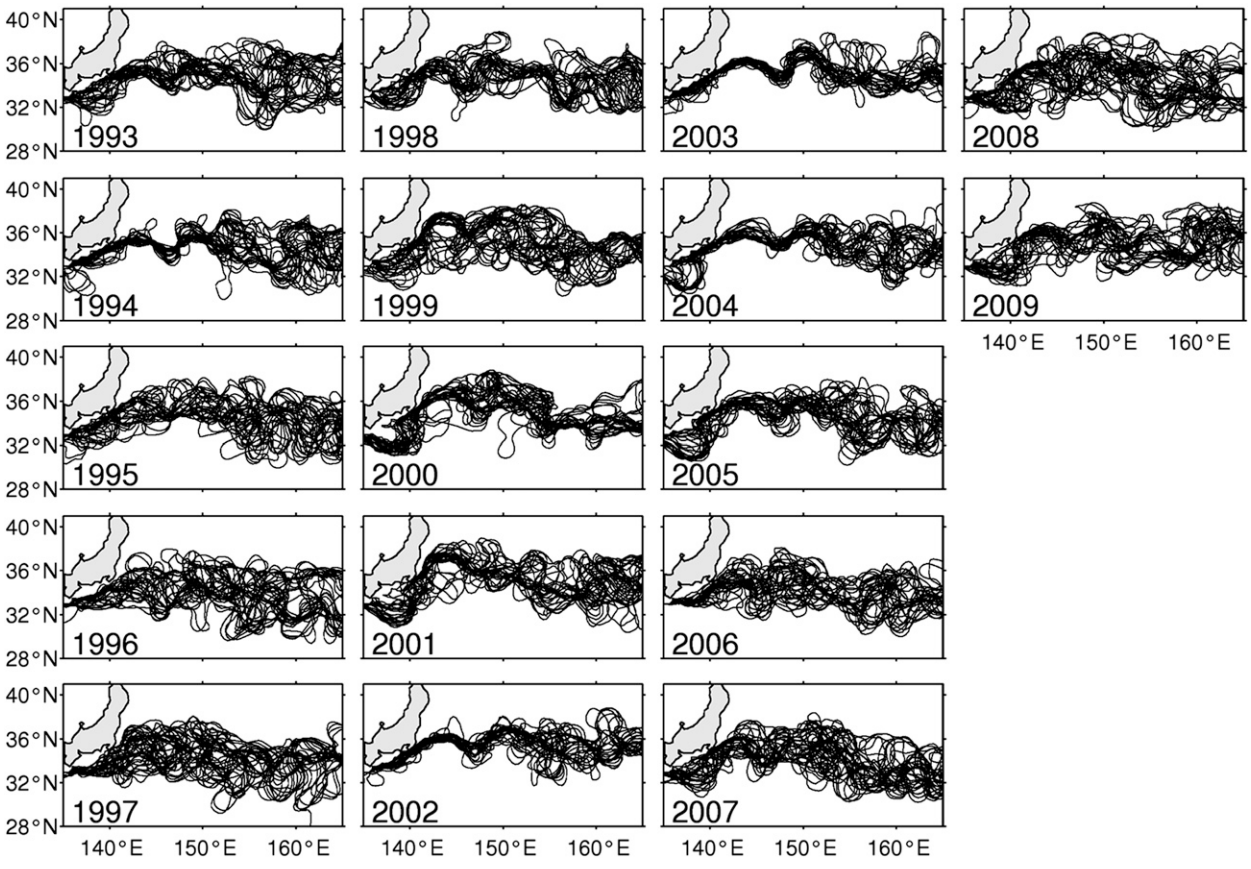

FIG. 5. Yearly paths of the Kuroshio and the Kuroshio Extension plotted every 14 days, as in Qiu and Chen (2005). (Figure courtesy of Bo Qiu, University of Hawaii at Manoa.)

or absorbing mesoscale eddies (Fig. 7). In association with this fluctuation, anticyclonic circulations constituting the southern recirculation gyre shift, repeatedly merging and separating, as described in Oka (2009). In late October to early November, the hydrographic lines of the KH-08-3 cruise leg 2 cross the Kuroshio Extension at five locations: near the western end of the 34°N line, 35°N of the 143°E line, and 33°30′, 34°, and 36°30′N of the 146°E line (Fig. 1). The southern portion of the hydrographic lines encompasses a cyclonic eddy centered at 29°20′N, 144°30′E. This eddy is centered at 29°N, 154°E in April, and subsequently moves westward (Fig. 7).

The hydrographic sections of the cruise cross the strong flow of the Kuroshio Extension at five locations similar to those on the altimetric sea surface height map (Fig. 8). The isothermal, isopycnal, and low-Q ($<2 \times 10^{-10}$ m^{-1} s^{-1}) structure of STMW is seen at depths of 100–500 dbar south of the Kuroshio Extension (east of 141°30′E in the 34°E section, south of 34°30′N in the 143°E section, south of 32°30′N in the 146°E section, and throughout the 27°30′ and 30°N sections), as well as in the isolated anticyclonic recirculation near 35°30′N in the 146°E section. The 27°30′N section also displays a relatively small but intense low-Q structure near 500 dbar, at 145°E. This is a patch of CMW trapped in a subsurface anticyclonic eddy, whose formation and migration were studied by Oka et al. (2009).

The permanent pycnocline south of the Kuroshio Extension exhibits undulations with a horizontal scale of 100–200 km, in addition to upward lifts at 28°50′N in the

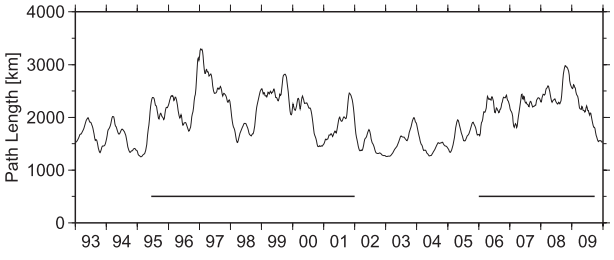

FIG. 6. Time series of the Kuroshio Extension pathlength integrated from 141° to 153°E, adapted from Qiu and Chen (2010). A three-month box filter was applied to the original, weekly data. Thick lines indicate the periods when the Kuroshio Extension is in a variable state.

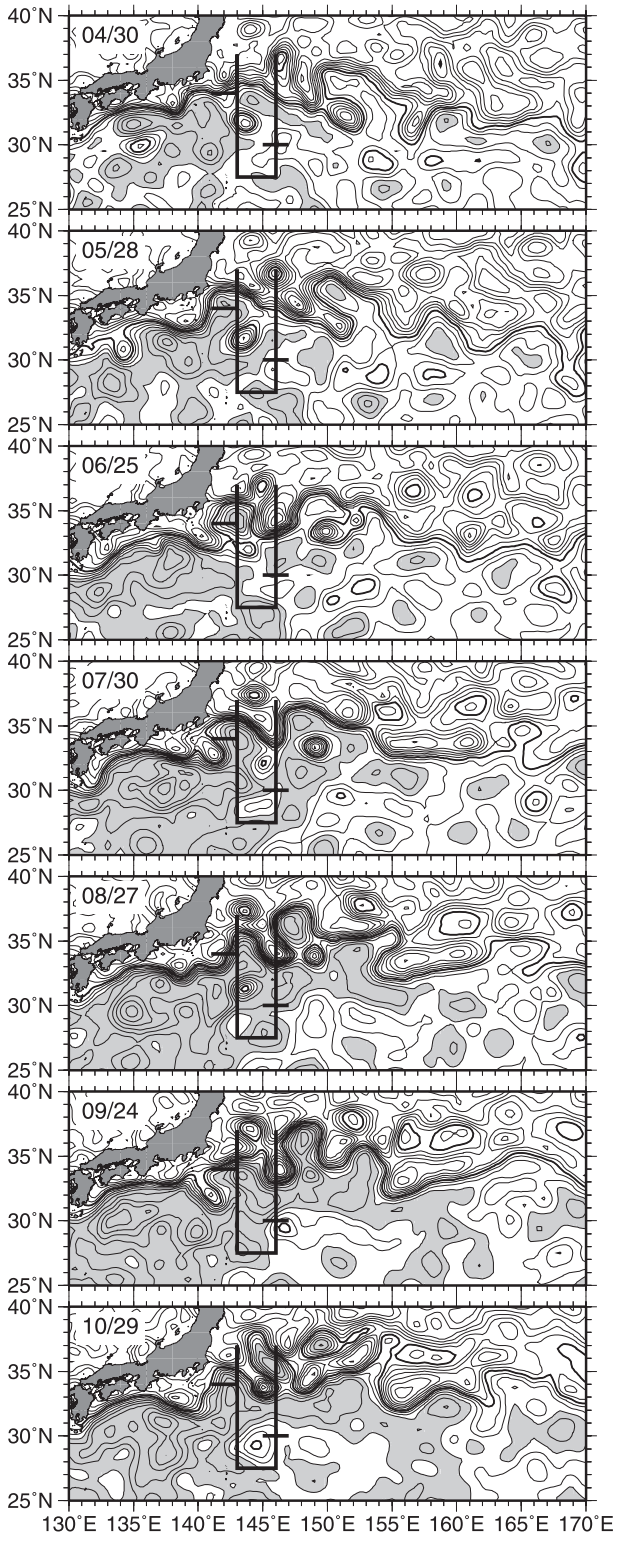

FIG. 7. Altimetric sea surface height maps southeast of Japan from 30 Apr through 29 Oct 2008, at a time interval of approximately 1 month, drawn as in Fig. 1. Thick black lines indicate the observation lines of the KH-08-3 cruise leg 2.

143°E section, at 30°10′N in the 146°E section, and at 145°E in the 30°N section associated with the cyclonic eddy (Fig. 9a). Specifically, the permanent pycnocline deepens at 142°40′E in the 34°N section; at 33°30′, 32°10′, 30°30′, and 29°30′N in the 143°E section; at 143°30′ and 146°E in the 27°30′N section; and at 32°20′N in the 146°E section, and becomes shallow in between. These mesoscale structures, particularly those in the 143°E section, are not fully resolved in the altimetric sea surface height map constructed using temporal and spatial interpolation (Fig. 1).

STMW also has mesoscale structure, existing as a sequence of patches with a horizontal scale of 100–200 km (Fig. 9c). Such mesoscale variation of STMW thickness is mainly determined by the variation of STMW bottom depth (Fig. 9b; correlation coefficient of 0.78), which in turn corresponds well to that of the permanent pycnocline depth (Fig. 9a; i.e., 0.83). In particular, the thickest portion of each STMW patch corresponds well to where the permanent pycnocline deepens (Fig. 9a). This strengthens the conclusions of the previous observational and modeling studies that thicker (thinner) STMW is preferentially formed in winter and distributed after spring in anticyclonic (cyclonic) mesoscale circulations/eddies where the permanent pycnocline is deeper (shallower), owing to weaker (stronger) background stratification and larger (smaller) oceanic heat loss in winter (Suga and Hanawa 1990; Uehara et al. 2003; Oka and Suga 2003; Pan and Liu 2005; Qiu et al. 2006; Rainville et al. 2007; Nishikawa et al. 2010; S. Kouketsu et al. 2011, manuscript submitted to *J. Oceanogr.*). The STMW top depth tends to increase northward (Fig. 9b), possibly because the upper portion of STMW at higher latitudes has been further eliminated owing to the earlier onset of cooling and the resultant deepening of the seasonal pycnocline (e.g., Qiu et al. 2006; Oka et al. 2011). This suggests that in order to examine the relation between the STMW structure and the mesoscale circulations, hydrographic observations along zonal lines are more preferable.

The core θ exhibits an apparent bimodal distribution (Figs. 9d and 10a), which coincides with the middle and cold modes observed by the Argo floats in spring (Fig. 3a, top panel). The western (eastern) hydrographic sections along 34°N, 143°E, and 27°30′N (146°E and 30°N) are occupied mainly by the middle (cold) mode, within which the cold (middle) mode exists with a relatively small scale (Fig. 9). Such intrusions of the different modes tend to occur at locations where the permanent pycnocline depth, the STMW bottom depth, and the STMW thickness reach their local maxima. This suggests that as the anticyclonic circulations south of the Kuroshio Extension gradually shift, repeatedly merging and separating (Fig. 7), they transport STMW zonally from the formation region to

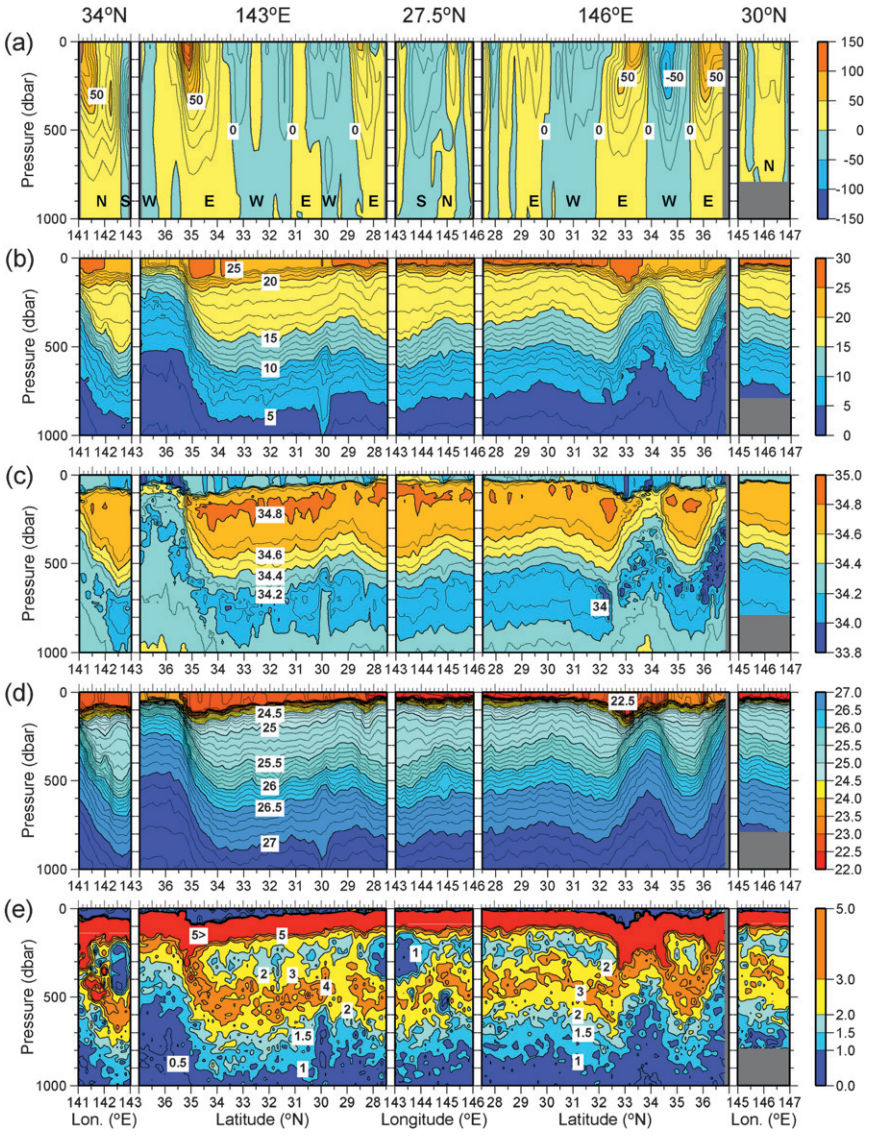

FIG. 8. Distributions of (a) geostrophic velocity (cm s^{-1}), (b) θ (°C), (c) S, (d) σ_θ (kg m^{-3}), and (e) Q (10^{-10} m^{-1} s^{-1}) in the hydrographic sections of the KH-08-3 cruise leg 2. Northward (eastward) velocity is exhibited for the zonal (meridional) sections, and "N," "S," "E," and "W" denote northward, southward, eastward, and westward flow, respectively, in (a). Contours are drawn at 0.5, 1, 1.5, 2, 3, 4, and 5 × 10^{-10} m^{-1} s^{-1} in (e). Long (short) ticks on the top of each indicate the locations of $CTDO_2$ (XCTD/XBT) stations.

a remote region. The most visible examples are two thick STMW patches observed near 34°N, 142°30′E and 27°30′N, 143°10′E (Figs. 8 and 9), which are associated with anticyclonic circulations centered at 33°N, 142°30′E and 28°N, 142°E, respectively (Fig. 1). Both patches are the cold mode embedded in the middle mode (Fig. 9), and are thought to be formed east of 150°E in late winter and subsequently transported westward (Fig. 4). On the basis of the monthly sea surface height maps (Fig. 7), we presume the following STMW circulation. The cold-mode STMW associated with these two patches is originally formed near 150°E, just south of the Kuroshio Extension in the late winter of 2008, and is trapped in an anticyclonic circulation centered at 31°N, 149°E in April. This circulation is broken into two circulations centered at 31°N, 149°E and 28°N, 148°E in June. Then, the northern circulation propagates westward and is absorbed by another anticyclonic circulation centered at 33°30′N, 143°30′E in September. The other one also migrates westward, to 28°N, 142°E, in October. In association with these shifts, the cold-mode STMW is transported westward. Similar transportation by anticyclonic circulations is expected to

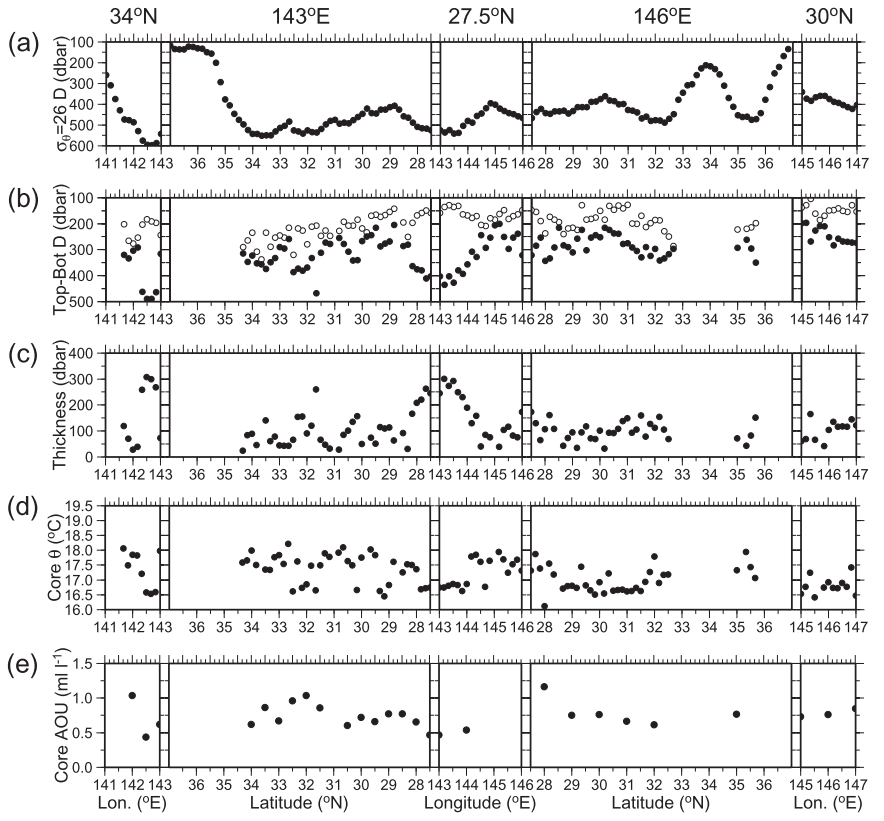

FIG. 9. Plots of (a) depth of the $\sigma_\theta = 26$ kg m^{-3} isopycnal representing the permanent pycnocline and (b) top (open circles) and bottom (closed circles) depths, (c) thickness, (d) core θ, and (e) core AOU of STMW against longitude or latitude at the hydrographic stations of the KH-08-3 cruise leg 2. Long (short) ticks on the top of each panel indicate the locations of $CTDO_2$ (XCTD/XBT) stations. Note that the depth increases downward along the ordinate in (a) and (b).

occur in other locations in the STMW formation region as well, stirring STMWs originated from different regions, as shown in Fig. 4.

The bimodal distribution of core θ is also observed by nearby Argo floats during the period of KH-08-3 cruise leg 2 (Fig. 10b), but not after that. In November–December the two modes are integrated to form one mode (Fig. 10c), as mentioned earlier, based on the float data from the entire STMW distribution region (Fig. 3a, bottom panel).

The core AOU is measured at the $CTDO_2$ stations at intervals of 30′ or 1° in latitude/longitude (Fig. 9e). It is negatively correlated with the STMW thickness, with a coefficient of −0.56 (Fig. 11), which implies that the core of a thicker STMW pycnostad associated with the deeper permanent pycnocline did not tend to dissipate since its formation. The lowest core AOU (0.44 ml l^{-1}) is associated with the thickest STMW, which is expected to have been the least dissipated. If we assume that this STMW pycnostad loses contact with the atmosphere at the end of March having an AOU of 0.1–0.2 ml l^{-1} (Suga and Hanawa 1990), the AOU increase of approximately 0.3 ml l^{-1} over 7 months yields an increase rate of 0.5 ml l^{-1} yr^{-1} owing almost purely to the oxygen consumption through the remineralization of organic matter. This value coincides with the rates obtained by Suga et al. (1989) and Oka and Suga (2005) for STMW in repeat hydrographic sections.

Our discussion so far assumes only one core (Q minimum) for each STMW pycnostad in a $CTDO_2$/XCTD/XBT/Argo profile. However, careful inspection reveals that some profiles have two or even three Q minima in the θ range of STMW (Fig. 12), as previously observed by Taneda et al. (2000). If we redefine the core as the Q minimum being less than 2.0×10^{-10} m^{-1} s^{-1} and having a magnitude of 0.3×10^{-10} m^{-1} s^{-1} in the θ range of 16°–19.5°C, permitting the existence of multiple cores, 24 STMW pycnostads out of 107 (22%) observed in the KH-08-3 cruise leg 2 have a second core, and 2 also have a third core. Similarly, 9 pycnostads out of 27 (33%) observed by the nearby Argo floats during the cruise period have a second core. These double or triple cores, when observed in the $CTDO_2$ profiles, are often accompanied by corresponding AOU minima (Fig. 12). Such a structure cannot be formed by

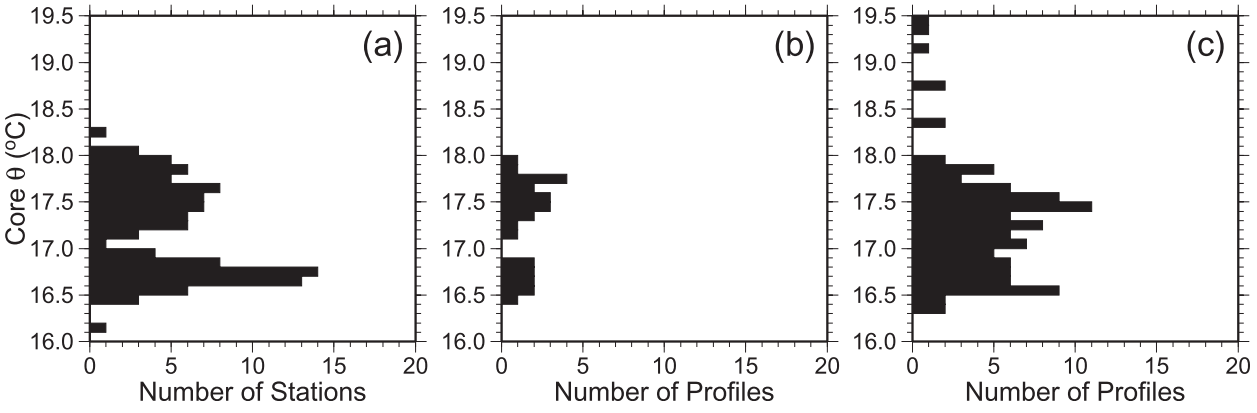

FIG. 10. Number of profiles with nonoutcropping STMW in each 0.1° bin of core θ based on (a) hydrographic data of the KH-08-3 cruise leg 2 and Argo float data at 25°–40°N, 140°–150°E on (b) 22 Oct–4 Nov 2008 and (c) 5 Nov–31 Dec 2008.

vertical processes (e.g., vertical mixing, the vertical shift of isopycnals due to internal waves) alone. Instead, it is likely to be formed owing to the interleaving of STMW pycnostads with different densities originating in different regions.

Actually, 17 out of 24 (71%) and 7 out of 9 (78%) pycnostads with double/triple cores based on the cruise and Argo data, respectively, have the first core of either the cold or middle mode and the second core of the other mode (Table 1). This indicates that after the middle and cold modes are stirred by mesoscale circulations (Fig. 4), they interleave with each other. Eventually, the two interleaving modes are expected to be vertically mixed with each other. This is a plausible explanation for the emergence of STMW with the intermediate core θ between the cold and middle modes in November–December (Figs. 3a and 10c).

5. Summary and discussion

Hydrographic data obtained by high-resolution shipboard observations and Argo floats have been analyzed to study the mesoscale structure and circulation of STMW. First, the STMW circulation over the entire distribution region in 2008 was examined by using the float data. In the late winter of 2008, STMW is formed in the zonally elongated anticyclonic recirculation between the Kuroshio Extension and 28°N, a region similar to the preceding winters. The core θ of the formed STMW clearly differs among regions; warm, middle, and cold modes of STMW with a core θ of approximately 18.8°, 17.7°, and 16.6°C are formed west of 140°E, between 140° and 150°E, and east of 150°E, respectively. After spring, the newly formed, thick STMW gradually shifts southward, decreasing in thickness. Simultaneously, the cold and middle modes of the STMW are gradually stirred, and finally coexist with each other in late fall. The two modes are also gradually mixed in terms of their properties. In November–December, they seem to be integrated to form a new mode having a core θ of approximately 17.2°C.

The observed STMW circulation in 2008 is much more turbulent than that in 2006 examined by Oka (2009). In 2006, STMW is formed in several anticyclonic circulations in the southern recirculation in late winter, and tends to be continually trapped in the respective circulations, remaining in the formation region until late fall. Such a difference between 2006 and 2008 is attributed to the Kuroshio Extension having a more variable path in 2008, which is associated with stronger eddy activities in the STMW formation region, which would enhance eddy transport of STMW during that year.

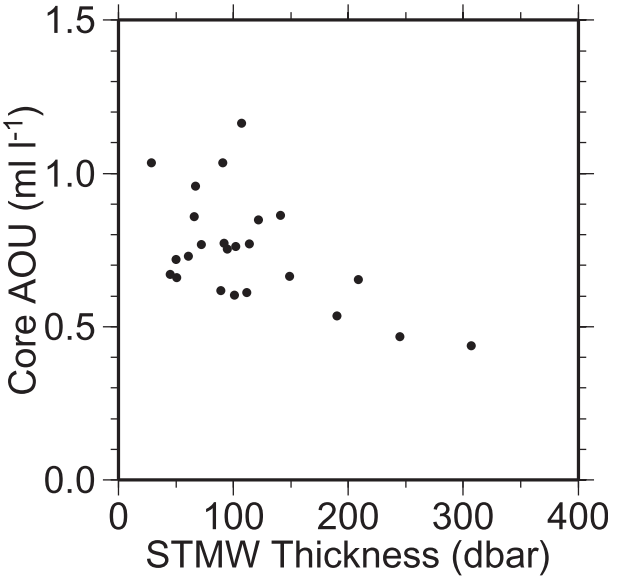

FIG. 11. Plots of core AOU against thickness for STMW at the hydrographic stations of the KH-08-3 cruise leg 2.

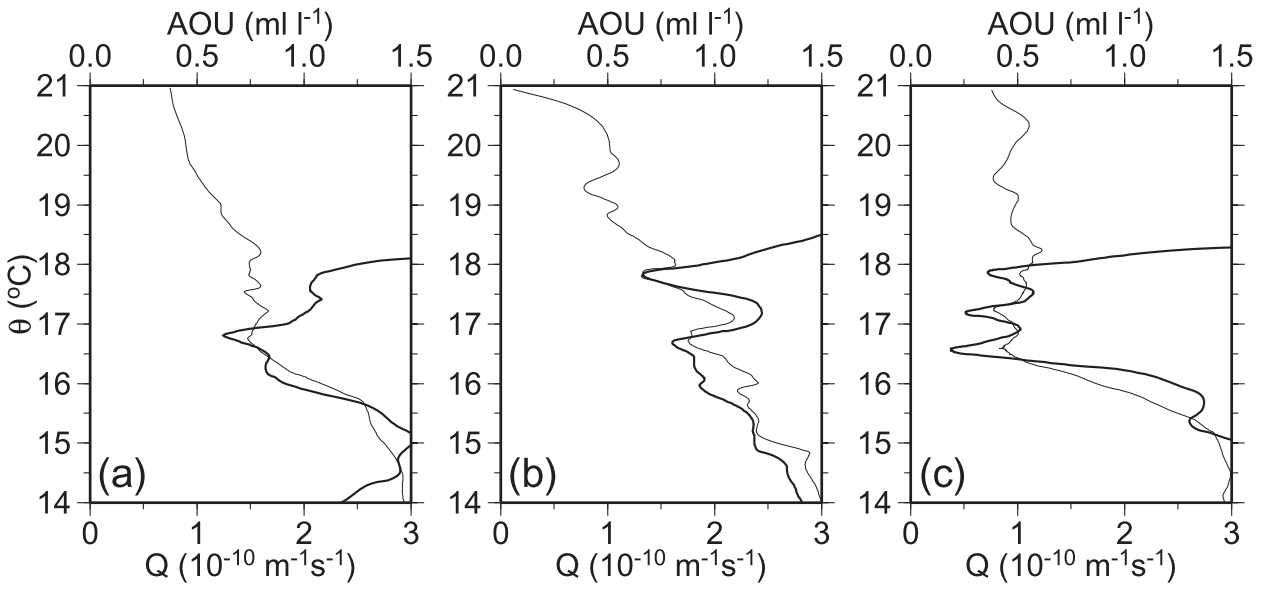

FIG. 12. Vertical profile of Q (thick curve) and AOU (thin curve) with respect to θ obtained at (a) 29°N, 146°E; (b) 29°30′N, 143°E; and (c) 34°N, 142°30′E during the KH-08-3 cruise leg 2. These are examples of single, double, and triple cores, respectively.

High-resolution shipboard observations were carried out in late October through early November 2008, along five zonal/meridional lines in the region of 27°30′–37°N, 141°–147°E, southeast of Japan. In the hydrographic sections, STMW exists south of the Kuroshio Extension as a sequence of patches with a horizontal scale of 100–200 km, and its thick portions determined by the bottom depth correspond well to the mesoscale deepening of the permanent pycnocline. The core θ of STMW in these sections is classified into two groups that coincide with the cold and middle modes observed by the Argo floats in spring. The western (eastern) part of the hydrographic sections are occupied mostly by the middle (cold) mode, within which the cold (middle) mode with a small horizontal scale exists, mostly at locations where the permanent pycnocline deepens and the STMW thickness attains a local maximum. Such a structure implies that as the mesoscale anticyclonic circulations south of the Kuroshio Extension gradually shift, repeatedly merging and separating, they transport each STMW patch away from its formation region, thereby stirring STMW patches that originated in different regions.

Further inspection of the hydrographic data from the cruise and those from the nearby Argo floats during the cruise period reveals that 20%–30% of the observed STMW pycnostads have 2 or 3 cores (Q minima), and most of the double cores have the core θ of the middle and cold modes. Such a structure is probably formed owing to the interleaving of the two modes after they are stirred by mesoscale circulations. We presume that the double cores are then vertically mixed to form the single core observed in November–December that has an intermediate core θ between the two modes.

The present study has verified that mesoscale transport of STMW occurs as previously demonstrated by the high-resolution ocean general circulation models (Rainville et al. 2007; Nishikawa et al. 2010) and that this horizontally mixes STMW originating from different regions when the Kuroshio Extension is in its highly variable state. It has been further suggested that such horizontal processes play an important role in destroying the vertically uniform structure of STMW after spring. The interleaving

TABLE 1. Number of hydrographic observations of the KH-08-3 cruise leg 2 and Argo float data at 25°–40°N, 140°–150°E from 22 Oct to 4 Nov 2008, classified by θ of the first and second cores of STMW pycnostads. 16.4°–17.1°C and 17.1°–18.2°C are the core θ of the cold and middle modes, respectively. Core θ higher than 18.2°C were not observed in either data.

KH-08-3 cruise leg 2 data			
	Second core		
First core	16.0°–16.4°C	16.4°–17.1°C	17.1°–18.2°C
16.0°–16.4°C	0	0	1
16.4°–17.1°C	4	0	9
17.1°–18.2°C	0	8	2
Argo float data			
	Second core		
First core	16.0°–16.4°C	16.4°–17.1°C	17.1°–18.2°C
16.0°–16.4°C	0	0	0
16.4°–17.1°C	0	0	3
17.1°–18.2°C	2	4	0

of STMW with different densities might occur in association with the dissipation of mesoscale anticyclonic circulations or eddies that have carried STMW away from its formation region. Submesoscale-resolving models are expected to be helpful in clarifying such smaller-scale processes.

The results from Oka (2009) and the present study suggest that not only the formation (Qiu and Chen 2006; Qiu et al. 2007) but also the circulation and dissipation of STMW are closely related to the decadal variability of the Kuroshio Extension system (Qiu and Chen 2005; Qiu et al. 2007). Since the Kuroshio Extension has returned to its stable state in 2010 (Qiu and Chen 2011), we expect to observe an STMW evolution distinct from that of 2008 in a few years by using the Argo float data that are much richer than the data available for the last period of stability (2002–04).

Acknowledgments. The authors are grateful to the captain, crew, and scientists participating in the KH-08-3 cruise leg 2 of R/V *Hakuho-maru* of the Japan Agency for Marine-Earth Science and Technology for their efforts in conducting the $CTDO_2$/XCTD/XBT measurements. They also thank Tsuyoshi Ohira for his assistance in preparing the Argo float data; Bo Qiu for providing the figures and data on the Kuroshio Extension variability; and Keita Iga, Shin-ichi Ito, and Bo Qiu for their insightful comments. Detailed comments from two anonymous reviewers enabled us to improve an early version of the manuscript. This work was partly supported by the Japan Society for Promotion of Science [KAKENHI, Grant-in-Aid for Scientific Research (B) 21340133], the Ministry of Education, Culture, Sports, Science and Technology, Japan [MEXT; Grant-in-Aid for Scientific Research in Priority Areas: ''Western Pacific Air-Sea Interaction Study (W-PASS)'' under Grant 21014004], the Agriculture, Forestry and Fisheries Research Council, Japan [AFFRC; ''Studies on Prediction and Application of Fish Species Alteration (SUPRFISH)''], and the Cooperative Program (142 in 2009) provided by the Ocean Research Institute, The University of Tokyo. The Argo float data used in this study were collected and made freely available by the International Argo Project and the national programs that contribute to it (see online at http://www.argo.ucsd.edu and http://argo.jcommops.org).

APPENDIX

XCTD Data Calibration

The S data of the KH-08-3 cruise leg 2 obtained by XCTD probes manufactured in 2006 and 2007 had a systematic negative bias of -0.05 to -0.1 compared to the data from $CTDO_2$, as previously reported by Kashino et al. (2009). On the other hand, those from the probes manufactured in 2008 did not appear to have a bias. Therefore, we added the following values as a function of θ to the S values from the problematic XCTD probes:

$$\begin{aligned}
\Delta S &= 0.01 + 0.04 \times \frac{\theta - 2}{6}, && \text{at} \quad 2^\circ \le \theta < 8^\circ\text{C};\\
&= 0.05 + 0.01 \times \frac{\theta - 8}{10}, && \text{at} \quad 8^\circ \le \theta < 18^\circ\text{C};\\
&= 0.06 + 0.02 \times \frac{\theta - 18}{3}, && \text{at} \quad 18^\circ \le \theta < 21^\circ\text{C}; \quad \text{and}\\
&= 0.08, && \text{at} \quad 21^\circ\text{C} \le \theta
\end{aligned} \tag{A1}$$

This procedure is believed to improve the S accuracy of XCTD measurements to ~0.03, which is comparable to the expected S accuracy of Argo profiling float measurements (less than 0.02; Oka and Ando 2004; Oka 2005).

REFERENCES

Akima, H., 1970: A new method of interpolation and smooth curve fitting based on local procedures. *J. Assoc. Comput. Methods,* **17,** 589–603.

Alexander, M. A., and C. Deser, 1995: A mechanism for the recurrence of wintertime midlatitude SST anomalies. *J. Phys. Oceanogr.,* **25,** 122–137.

Aoki, Y., T. Suga, and K. Hanawa, 2002: Subsurface subtropical fronts of the North Pacific as inherent boundaries in the ventilated thermocline. *J. Phys. Oceanogr.,* **32,** 2299–2311.

Argo Data Management Team, 2009: Argo quality control manual, version 2.5. Argo Data Management, 39 pp. [Available online at http://www.argodatamgt.org/.]

Bates, N. R., A. C. Pequignet, R. J. Johnson, and N. Gruber, 2002: A variable sink for atmospheric CO_2 in subtropical mode water of the North Atlantic Ocean. *Nature,* **420,** 489–493.

Bretherton, F. P., R. E. Davis, and C. B. Fandry, 1976: A technique for objective analysis and design of oceanographic experiment applied to MODE-73. *Deep-Sea Res.,* **23,** 559–582.

Ducet, N., P. Y. Le Traon, and G. Reverdin, 2000: Global high-resolution mapping of ocean circulation from TOPEX/Poseidon and *ERS-1* and *-2*. *J. Geophys. Res.,* **105,** 19 477–19 498.

Gu, D., and S. G. H. Philander, 1997: Interdecadal climate fluctuations that depend on exchanges between the tropics and extratropics. *Science,* **275,** 805–807.

Hanawa, K., and J. Kamada, 2001: Variability of core layer temperature (CLT) of the North Pacific Subtropical Mode Water. *Geophys. Res. Lett.,* **28,** 2229–2232.

——, and S. Sugimoto, 2004: 'Reemergence' areas of winter sea surface temperature anomalies in the world's oceans. *Geophys. Res. Lett.,* **31,** L10303, doi:10.1029/2004GL019904.

Hasumi, H., H. Tatebe, T. Kawasaki, M. Kurogi, and T. T. Sakamoto, 2010: Progress of North Pacific modeling over the past decade. *Deep-Sea Res. II,* **57,** 1188–1200.

Kashino, Y., N. España, F. Syamsudin, K. J. Richards, T. Jensen, P. Dutrieux, and A. Ishida, 2009: Observations of the North Equatorial Current, Mindanao Current, and Kuroshio Current System during the 2006/07 El Niño and 2007/08 La Niña. *J. Oceanogr.,* **65,** 325–333.

Kobashi, F., H. Mitsudera, and S.-P. Xie, 2006: Three subtropical fronts in the North Pacific: Observational evidence for mode water-induced subsurface frontogenesis. *J. Geophys. Res.,* **111,** C09033, doi:10.1029/2006JC003479.

——, S.-P. Xie, N. Iwasaka, and T. T. Sakamoto, 2008: Deep atmospheric response to the North Pacific oceanic subtropical front in spring. *J. Climate,* **21,** 5960–5975.

Kubokawa, A., 1999: Ventilated thermocline strongly affected by a deep mixed layer: A theory for subtropical countercurrent. *J. Phys. Oceanogr.,* **29,** 1314–1333.

——, and T. Inui, 1999: Subtropical countercurrent in an idealized ocean GCM. *J. Phys. Oceanogr.,* **29,** 1303–1313.

Ladd, C. A., and L. Thompson, 2000: Formation mechanisms for North Pacific central and eastern subtropical mode waters. *J. Phys. Oceanogr.,* **30,** 868–887.

Latif, M., and T. P. Barnett, 1994: Causes of decadal climate variability over the North Pacific and North America. *Science,* **266,** 634–637.

Masumoto, Y., 2010: Sharing the results of a high-resolution ocean general circulation model under a multi-discipline framework—A review of OFES activities. *Ocean Dyn.,* **60,** 633–652.

Masuzawa, J., 1969: Subtropical Mode Water. *Deep-Sea Res.,* **16,** 463–472.

Nakamura, H., 1996: A pycnostad on the bottom of the ventilated portion in the central subtropical North Pacific: Its distribution and formation. *J. Oceanogr.,* **52,** 171–188.

Nishikawa, S., and A. Kubokawa, 2007: Mixed layer depth front and subduction of low potential vorticity water in an idealized ocean GCM. *J. Oceanogr.,* **63,** 125–134.

——, H. Tsujino, K. Sakamoto, and H. Nakano, 2010: Effects of mesoscale eddies on subduction and distribution of Subtropical Mode Water in an eddy-resolving OGCM of the western North Pacific. *J. Phys. Oceanogr.,* **40,** 1748–1765.

Oka, E., 2005: Long-term sensor drift found in recovered Argo profiling floats. *J. Oceanogr.,* **61,** 775–781.

——, 2009: Seasonal and interannual variation of North Pacific Subtropical Mode Water in 2003–2006. *J. Oceanogr.,* **65,** 151–164.

——, and T. Suga, 2003: Formation region of North Pacific subtropical mode water in the late winter of 2003. *Geophys. Res. Lett.,* **30,** 2205, doi:10.1029/2003GL018581.

——, and K. Ando, 2004: Stability of temperature and conductivity sensors of Argo profiling floats. *J. Oceanogr.,* **60,** 253–258.

——, and T. Suga, 2005: Differential formation and circulation of North Pacific Central Mode Water. *J. Phys. Oceanogr.,* **35,** 1997–2011.

——, L. D. Talley, and T. Suga, 2007: Temporal variability of winter mixed layer in the mid- to high-latitude North Pacific. *J. Oceanogr.,* **63,** 293–307.

——, K. Toyama, and T. Suga, 2009: Subduction of North Pacific central mode water associated with subsurface mesoscale eddy. *Geophys. Res. Lett.,* **36,** L08607, doi:10.1029/2009GL037540.

——, S. Kouketsu, K. Toyama, K. Uehara, T. Kobayashi, S. Hosoda, and T. Suga, 2011: Formation and subduction of Central Mode Water based on profiling float data, 2003–08. *J. Phys. Oceanogr.,* **41,** 113–129.

Pan, A., and Q. Liu, 2005: Mesoscale eddy effects on the wintertime vertical mixing in the formation region of the North Pacific Subtropical Mode Water. *Chin. Sci. Bull.,* **50,** 1949–1956.

Qiu, B., 2002: The Kuroshio Extension system: Its large-scale variability and role in the midlatitude ocean-atmosphere interaction. *J. Oceanogr.,* **58,** 57–75.

——, and S. Chen, 2005: Variability of the Kuroshio Extension jet, recirculation gyre, and mesoscale eddies on decadal timescales. *J. Phys. Oceanogr.,* **35,** 2090–2103.

——, and ——, 2006: Decadal variability in the formation of the North Pacific Subtropical Mode Water: Oceanic versus atmospheric control. *J. Phys. Oceanogr.,* **36,** 1365–1380.

——, and ——, 2010: Eddy-mean flow interaction in the decadally modulating Kuroshio Extension system. *Deep-Sea Res. II,* **57,** 1098–1110.

——, and ——, 2011: Effect of decadal Kuroshio Extension jet and eddy variability on the modification of North Pacific Intermediate Water. *J. Phys. Oceanogr.,* **41,** 503–515.

——, P. Hacker, S. Chen, K. A. Donohue, D. R. Watts, H. Mitsudera, N. G. Hogg, and S. R. Jayne, 2006: Observations of the Subtropical Mode Water evolution from the Kuroshio Extension System Study. *J. Phys. Oceanogr.,* **36,** 457–473.

——, S. Chen, and P. Hacker, 2007: Effect of mesoscale eddies on subtropical mode water variability from the Kuroshio Extension System Study (KESS). *J. Phys. Oceanogr.,* **37,** 982–1000.

Rainville, L., S. R. Jayne, J. L. McClean, and M. E. Maltrud, 2007: Formation of subtropical mode water in a high-resolution ocean simulation of the Kuroshio Extension region. *Ocean Modell.,* **17,** 338–356.

Roemmich, D., and Coauthors, 2001: Argo: The global array of profiling floats. *Observing the Oceans in the 21st Century,* C. J. Koblinsky and N. R. Smith, Eds., GODAE Project Office, Bureau of Meteorology, 248–258.

Suga, T., and K. Hanawa, 1990: The mixed layer climatology in the northwestern part of the North Pacific subtropical gyre and the formation area of Subtropical Mode Water. *J. Mar. Res.,* **48,** 543–566.

——, and ——, 1995a: Interannual variations of North Pacific Subtropical Mode Water in the 137°E section. *J. Phys. Oceanogr.,* **25,** 1012–1017.

——, and ——, 1995b: The subtropical mode water circulation in the North Pacific. *J. Phys. Oceanogr.,* **25,** 958–970.

——, ——, and Y. Toba, 1989: Subtropical mode water in the 137°E section. *J. Phys. Oceanogr.,* **19,** 1605–1618.

——, Y. Takei, and K. Hanawa, 1997: Thermostad distribution in the North Pacific subtropical gyre: The central mode water and the subtropical mode water. *J. Phys. Oceanogr.,* **27,** 140–152.

——, K. Motoki, and K. Hanawa, 2003: Subsurface water masses in the central North Pacific transition region: The repeat section along the 180° meridian. *J. Oceanogr.,* **59,** 435–444.

——, ——, Y. Aoki, and A. M. Macdonald, 2004: The North Pacific climatology of winter mixed layer and mode waters. *J. Phys. Oceanogr.,* **34,** 3–22.

Sugimoto, S., and K. Hanawa, 2005: Remote reemergence areas of winter sea surface temperature anomalies in the North

Pacific. *Geophys. Res. Lett.,* **32,** L01606, doi:10.1029/2004GL021410.

——, and ——, 2010: Impact of Aleutian Low activity on the STMW formation in the Kuroshio recirculation gyre region. *Geophys. Res. Lett.,* **37,** L03606, doi:10.1029/2009GL041795.

Taneda, T., T. Suga, and K. Hanawa, 2000: Subtropical mode water variation in the southwestern part of the North Pacific subtropical gyre. *J. Geophys. Res.,* **105,** 19 591–19 598.

Tsujino, H., and T. Yasuda, 2004: Formation and circulation of mode waters of the North Pacific in a high-resolution GCM. *J. Phys. Oceanogr.,* **34,** 399–415.

Uehara, H., T. Suga, K. Hanawa, and N. Shikama, 2003: A role of eddies in formation and transport of North Pacific Subtropical Mode Water. *Geophys. Res. Lett.,* **30,** 1705, doi:10.1029/2003GL017542.

Yasuda, T., and K. Hanawa, 1997: Decadal changes in mode waters in the midlatitude North Pacific. *J. Phys. Oceanogr.,* **27,** 858–870.